

Electronic supplementary information for the research article “Label-free Enrichment of Human Adipose-Derived Stem Cells using a Continuous Microfluidic Sorting Cascade”

2.1.2 Design of the DLD microfluidic sorter

Multiple sets of slanted micro-posts arrays were designed with cut-off critical diameter (D_c) of 16.4, 18.4, and 20.4 μm . We chose this set of cut-off critical diameters based on the size difference between ADSC and ADSC-depleted SVF cell sub-population, which was characterized using a hemocytometer in Section 3.1 in the main article. Accordingly, the design parameters and geometrical arrangement of the micro-post arrays were implemented (Figure S1 and Table S1) as the follows:

$$D_c = 1.4G_l\varepsilon^{0.48} \quad (1)$$

$$\varepsilon = \frac{(G_d + D_p)\tan\theta}{G_l + D_p} \quad (2)$$

$$\varepsilon' = \tan\theta \quad (3)$$

where D_c is the critical diameter, D_p is the micro-post diameter, G_l is the lateral gap distance, G_d is the downstream gap distance, ε is the modified slope of the micro-posts array, ε' is the actual slope of the micro-posts array, and θ is the actual slanted angle of the micro-posts array.

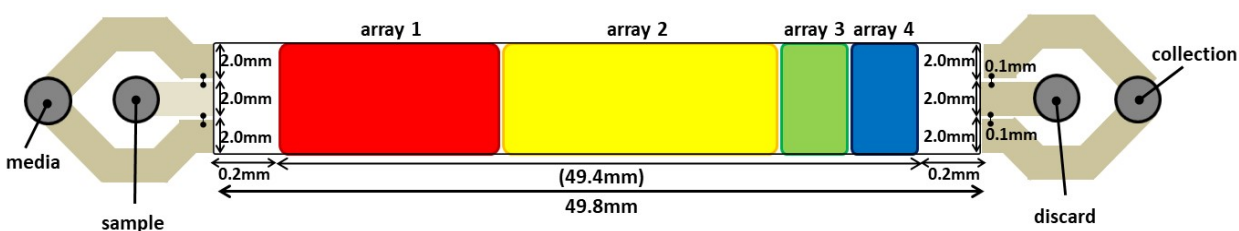


Figure S1. Arrangement of micro-post arrays and inlets/outlets design for DLD microfluidic sorter for ADSCs and SVF-cell mixture.

Table S1. Design parameters for DLD microfluidic sorter for ADSCs and SVF cell mixture separation

array no.	ε	D_c	$\Delta\lambda$	ΔD_c	no. of pillars	total lateral displacement	total length	design parameters	D_p	G_d	G_l	ε' (tan θ)	in μm
1	0.01133	16.3012	1.7		176	299.2	17600		50	50	100	0.017	
2	0.048	16.2965	4.8	-0.0047	230	1104	23000		50	50	50	0.048	
3	0.062	18.4266	6.2	2.13015	48	297.6	4800		50	50	50	0.062	
4	0.077	20.4462	7.7	2.01961	40	308	4000		50	50	50	0.077	
total						2008.8	49400						

The symmetric design of slanted DLD micro-posts arrays on two sides of each DLD microfluidic sorter increased the throughput rate by two-fold. We designed the channel height as 40 μm , and the entire channel width was 6mm. The micro-posts diameter was designed to be 50 μm with downstream gap size of 50 μm . The lateral gap size was designed as 50 μm , except for the first array which is 100 μm . We implemented an asymmetrical arrangement of the micro-post array in the upstream region of the DLD microfluidic sorter to reduce cell clogging problem [1]. In this arrangement, the lateral gap was designed to be larger than the downstream gap, such that cells traversing the micro-posts have less chance to collide with lateral micro-posts and get stuck between lateral micro-posts (Figure S2).

Figure S2. The arrangement of DLD cell sorter: asymmetric DLD micro-post gap-size ratio implementation.

The total length span of the DLD micro-posts arrays was 49.4mm. The inlet closest to the centerline was for cell sample input. The other inlet connecting to the side of the channel was for the culture media input to create sheath flow. The width of the sheath inlet was approximately twice that of the sample inlet. The width of the collect outlet was twice that of the discard outlet. In normal operation, the sheath flow rate was roughly twice the sample flow rate, resulting in 2 times dilution factor. The expected accumulation of lateral displacement of target cells ADSCs was 2mm.

The geometry of collect and discard outlet channels was designed to accommodate alteration of cell recovery characteristics near the outlets due to the difference of fluidic resistance. In laminar incompressible channel flow, for a rectangular cross section with a width w and a height h and the geometric constraint $h < w$, the fluidic resistance can be calculated as follows:

$$R_h \approx \frac{12\mu L}{wh^3(1 - 0.630h/w)} \quad (4)$$

where μ is the fluid dynamic viscosity, L is the channel length, w is the channel width, and h is the channel height.

2.1.3 Device fabrication process

Different parts of the DLD microfluidic device after fabrication was imaged under optical microscopy with phase imaging in Figure S3.

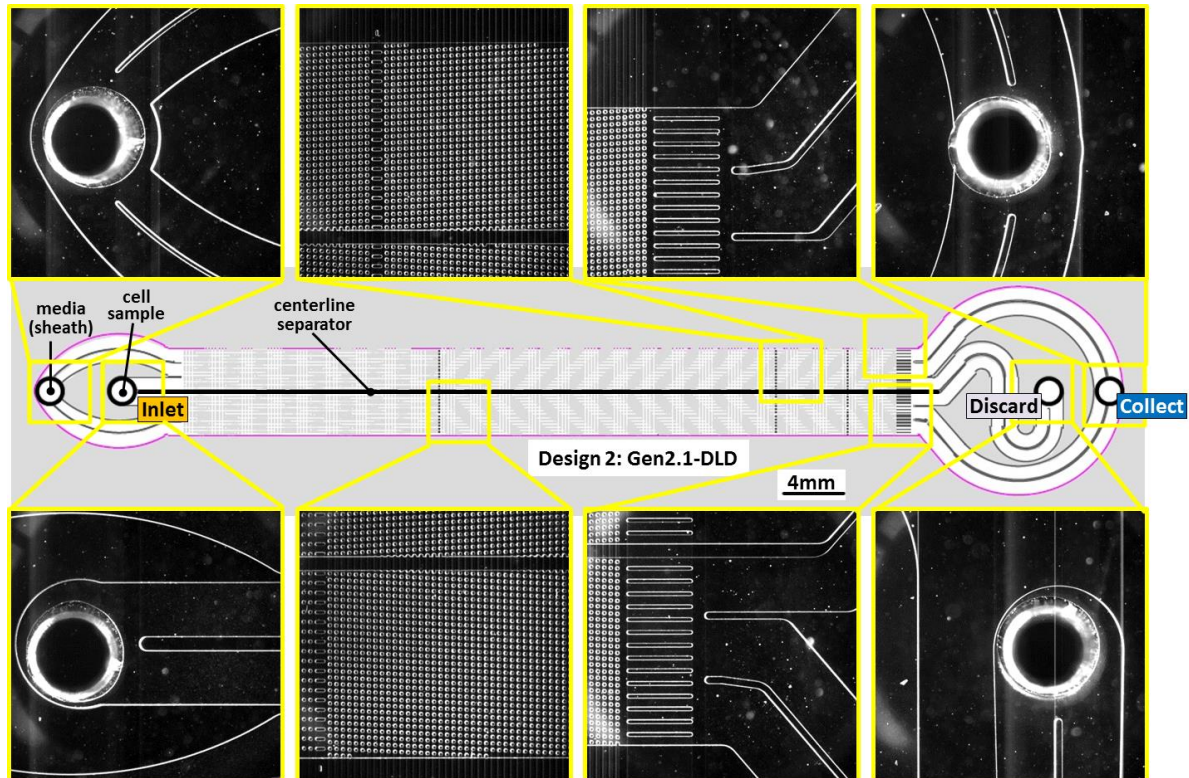


Figure S3. Micro-post arrays-based DLD microfluidic sorter for ADSC sorting. The microfluidic device has symmetrical arrangement of slanted micro-post arrays, in which the throughput rate was doubled. Device imaged with phase imaging under an optical microscope.

The spiral inertial microfluidic sorter device had wider channels without microscopic patterns. A picture of the device is shown in Figure 2a in the main article.

2.3.4 Continuous microfluidic sorter cascade

Optimization of DLD microfluidic sorters

We first optimized the performance of the DLD microfluidic sorter alone. The flow resistance ratio between the collect and discard outlets affected cell or particle recovery. As an initial trial, we prepared 10.3 μ m Nile Red fluorescent micro-particles (Spherotech, Inc.) suspension, which was then driven into the DLD

microfluidic device with flow rates at 40 μ L/min (sample) and 80 μ L/min (sheath), using two separate syringe pumps (Harvard Apparatus). When examining the fluorescent flow trajectories of 10.3 μ m Nile Red micro-particles under the epifluorescence microscope (Nikon TiE) near the outlets of DLD microfluidic sorter, we observed that the flow tracers tended to skew towards the discard outlet along the centerline (Figure S4). We also found that the sample volume collected in the discard outlet was about twice that from the collect outlet, which was opposite to the expected volume ratio of recovery in our design. This was attributed to the length of microfluidic channels in each arm of the collect outlet being longer than that of the discard outlet. Thus, flow resistance of the discard outlet was lower than that of the collect outlet, resulting in larger flow volume towards the discard outlet. Although it seemed to be desirable to collect more small cells/particles (ADSC-depleted SVF sub-population) at the discard outlet, it also possibly diverted targeted ADSCs towards the discard outlet, leading to low ADSC recovery.

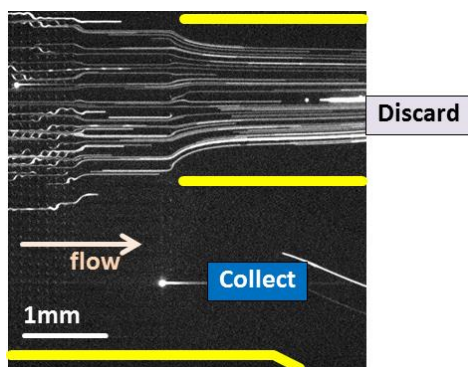


Figure S4. Fluorescent flow trace of 10.3 μ m Nile Red fluorescent micro-particles near the DLD microfluidic sorter under 40 μ L/min (cell sample inlet) and 80 μ L/min (media, sheath inlet).

We further demonstrated the tunability of outlet flow resistance, R_h by inserting a microfluidic control valve to the connection tubing of the discard outlet. The microfluidic control valve was enabled by a screw knob which varied the fluid flow rate through the tubing. Using a syringe pump (Harvard Apparatus), a suspension of 10.3 μ m Nile Red fluorescent micro-particles was driven to the DLD microfluidic sorter with flow rates at 40 μ L/min (sample) and 80 μ L/min (sheath). In Figure S5a, when the hydrodynamic resistance at the discard outlet was much larger than the collect outlet, the fluorescence micro-particles flow trace appeared like an expansion. As we gradually decreased the hydrodynamic flow resistance in the discard outlet, the flow trace expansion tended to be reduced as shown in Figure S5b. When we further decreased the flow resistance, the fluorescent micro-particles flow trajectories pinched into the discard outlet in Figure S5c, similar to results in Figure S4, in which no fluidic resistance was added to the discard outlet tubing.

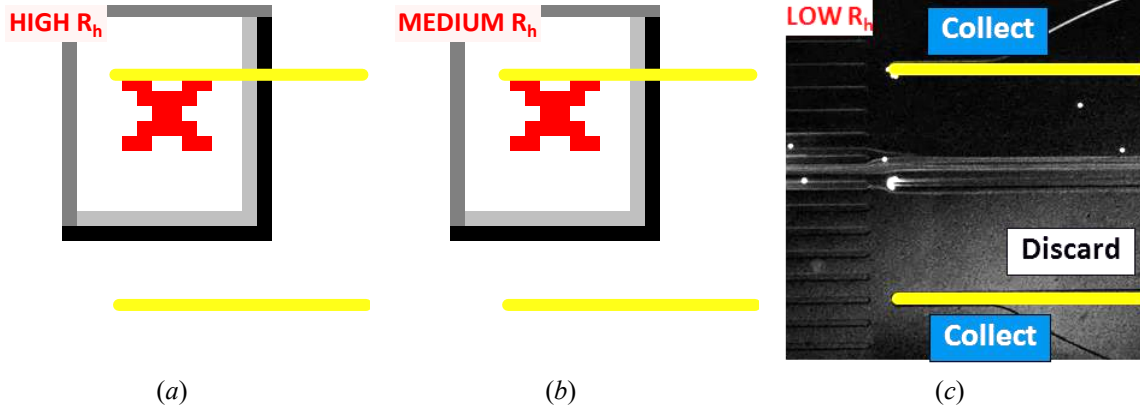


Figure S5. Tunability of flow resistance in the outlet recovery: (a) R_h at discard outlet $\gg R_h$ at collect outlet, (b) R_h at discard outlet $> R_h$ at collect outlet and (c) R_h at discard outlet $\sim R_h$ at collect outlet.

For circular channel with cross-section of radius r , the fluidic resistance can be calculated as follows:

$$R_h = \frac{8\mu L}{\pi r^4} \quad (5)$$

After a simple calculation based on equation (4) and (5), to compensate for the outlet length difference, a small Tygon™ tubing (with an inner diameter of 0.010" and a length of 2 cm) was inserted to the discard outlet to balance the recovery.

Next, we briefly investigated the effect of the flow rate on the sorting performance on the DLD microfluidic sorter. A pure population of cultured ADSCs at a concentration about 5×10^5 cells/mL without staining flowed through the DLD microfluidic sorter at a volume flow rate ratio of 1:2 (cell sample: sheath media) by syringe pump (Harvard Apparatus). The small Tygon™ tubing (with an inner diameter of 0.010" and a length of 2cm) inserted into the discard outlet to match the outlet flow resistance with the collect outlet. Thus, the flow traces of ADSCs appeared to be roughly horizontal and not diverted to either collect or discard outlets under optical phase imaging (Figure S6a). Then, we counted individual traces of ADSCs collected by the outlets and determined the ADSC recovery ratio at different throughputs in Figure S6b. We found that at flow rates of 80 $\mu\text{L}/\text{min}$ (cell sample) and 160 $\mu\text{L}/\text{min}$ (media, sheath), the ADSC recovery was about 77%, which was similar to flow rates of 40 $\mu\text{L}/\text{min}$ (cell sample) and 80 $\mu\text{L}/\text{min}$ (media, sheath). ADSC recovery dropped to 61% when we increased the flow rates to 160 $\mu\text{L}/\text{min}$ (cell sample) and 320 $\mu\text{L}/\text{min}$ (media, sheath). The degradation of ADSC recovery was attributed to cell deformability. With higher flow rates, ADSCs experienced high mechanical stress, short residence time, and cell deformation. The apparent diameter of ADSCs became smaller. The deformed ADSCs traversed the slanted micro-post

arrays in a “zigzag” manner and were collected in discard outlet, resulting in less accumulative lateral deflection and reducing targeted ADSC recovery in the collect outlet at the side.

With all above implementations, we had briefly determined the operating conditions and flow rates for the DLD microfluidic sorter to optimize ADSC collection in the side collect outlet. Further fine-tuning of its operation in the microfluidic sorter cascade which contained the spiral inertial microfluidic sorter and a Y-splitter device will be explained in the following section.

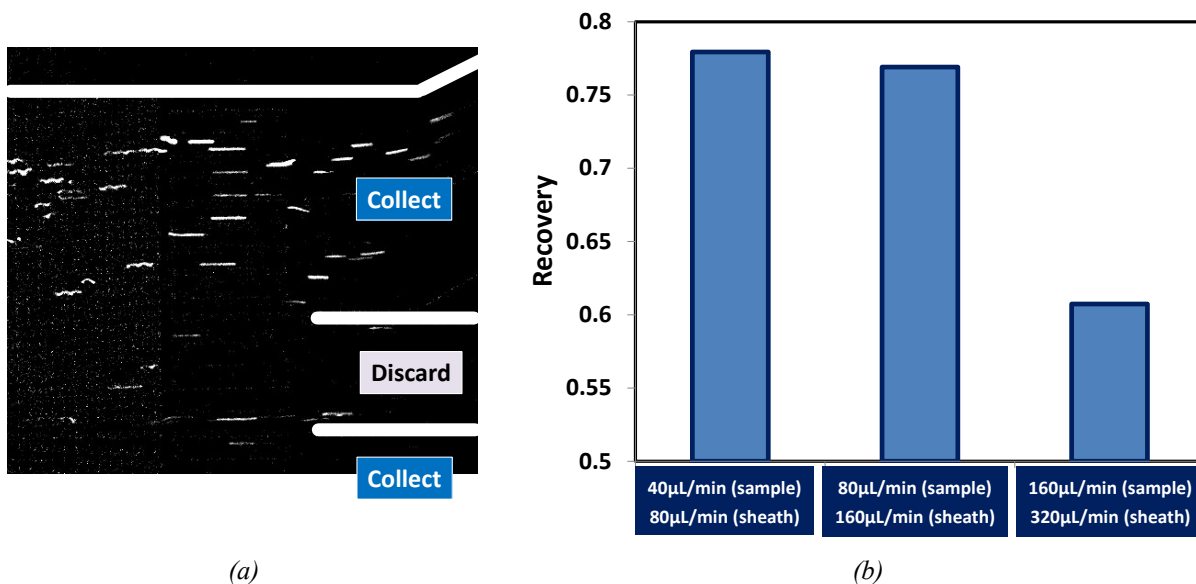


Figure S6. ADSC recovery in DLD microfluidic sorter: (a) flow trace by optical microscopy and (b) recovery at different throughput rates

Optimization of continuous microfluidic sorter cascade

The microfluidic sorter cascade was assembled as described in Figure 2 in the main article. We determined the optimized flow conditions for both spiral inertial and DLD microfluidics sorters in several steps. The ADSCs stained with CellTracker™ Green were mixed with 2 μm red fluorescent microspheres to enable flow visualization. We used 2 μm red fluorescent microspheres as the flow tracer, and not for sorting performance characterization purpose. The small microspheres enabled precise real-time visualization and fine-tuning of hydrodynamic focusing in the inlet region of the DLD microfluidic sorters and reduced the chance of clogging for prolonged usage of the DLD microfluidic sorters in flow condition optimization. Upon several iterations of fine tuning of the operational parameters, we determined the optimal working conditions with inlet sample flow rate of the inertial microfluidic sorter at 500 μL/min and the sheath flows

of each DLD microfluidic sorter at 200 μ L/min. The flow trajectories of both CellTracker™ Green stained ADSCs and 2 μ m red fluorescent microspheres in the spiral inertial microfluidic sorter at inlet sample rate of 500 μ L/min were imaged under an epifluorescence microscope (Nikon TiE with Andor iXon EMCCD camera) with an exposure time of 500ms (Figure S7). The ADSCs were hydrodynamically focused into the collect outlet channel of the spiral inertial microfluidic sorter. Dominated by Dean vortex secondary flow in the spanwise direction, the fluorescent flow trajectories of the 2 μ m red fluorescent microspheres spread across the channel width. No backflow was observed in outlet region of the spiral inertial microfluidic sorter by inserting the 20 cm long 0.010" inner diameter Tygon™ flow restrictor to the discard outlet of the spiral inertial microfluidic sorter to balance the fluidic resistance with the collect outlet. Both flow trajectories of ADSCs (green) and 2 μ m red fluorescent microspheres were stable.

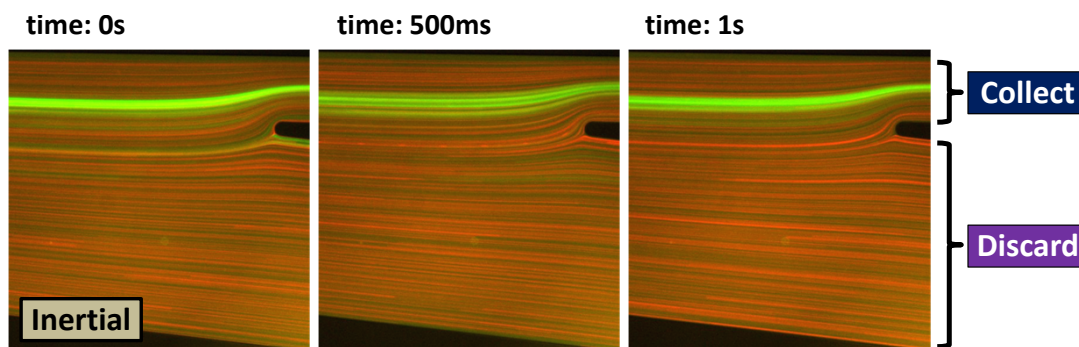


Figure S7. Optimized sorting/recovery of ADSCs (green) spiked in 2 μ m red fluorescent microspheres near the outlet region of the spiral inertial sorter in the continuous microfluidic sorter cascade under an inlet flow rate of 500 μ L/min. Several images were taken at successive time steps.

Mismatch in flow rate ratio between the sheath and sample inlets can result in “squeezing” or “expansion” of the sample flow stream close to the inlets in DLD microfluidic sorters. In Figure S8, at the sheath flow rate 200 μ L/min, the 2 μ m red fluorescent microspheres near the inlet region of the DLD microfluidic sorters were hydrodynamically focused by sheath flows without any expansion, constriction or distortion. This indicated that we have matched the collect outlet flow rate of the spiral inertial microfluidic sorter with this sheath flow rate of each DLD microfluidic sorter. In addition, this sheath flow rate was only 25% higher than the single DLD microfluidic sorter characterization, which should not cause significant degradation to the device performance in ADSC recovery. The 2 μ m microspheres migrated horizontally and interacted with slanted micro-post arrays in “zigzag” flow paths in the DLD microfluidic sorters.

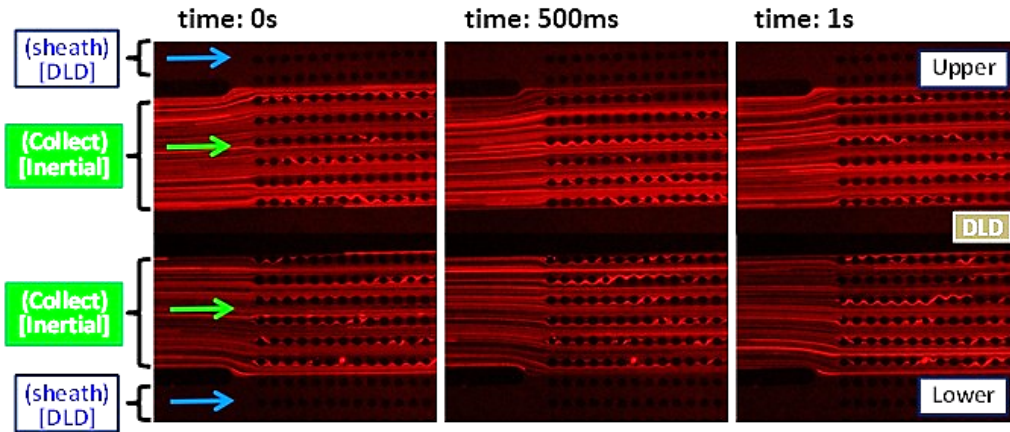


Figure S8. Optimized hydrodynamic focusing of $2\mu\text{m}$ red fluorescent microspheres in the inlet region of the DLD microfluidic sorter in the microfluidic sorter cascade under sheath flow rate of $200\mu\text{L}/\text{min}$. Several Images were taken at successive time steps.

3.1 Size Distribution of ADSC and ADSC-depleted SVF Cell Sub-population

The size distribution of three sub-populations of ADSC, SVF, and ADSC-depleted SVF with Student's t test result was shown in Figure S9.

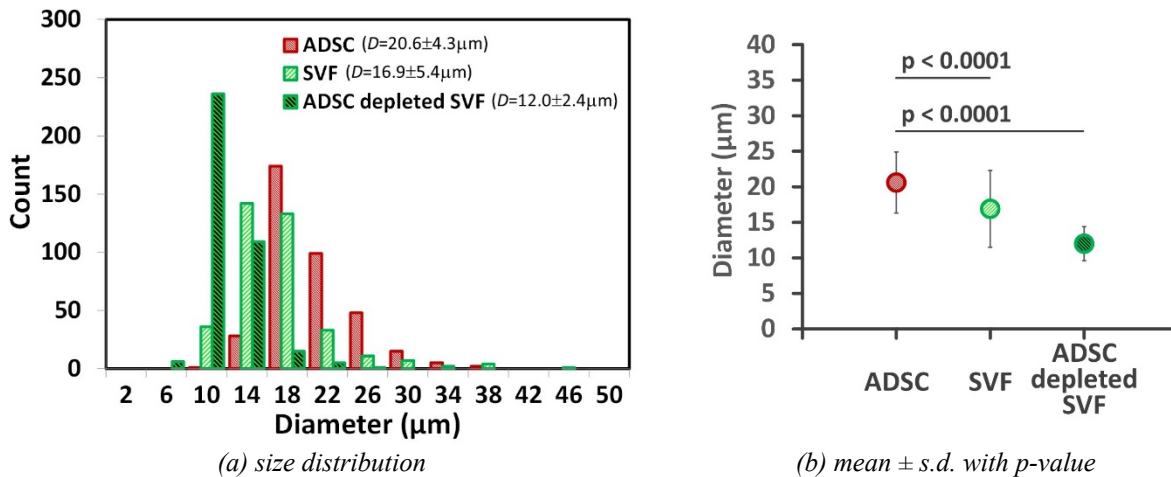


Figure S9. Size characterization of ADSCs, SVF cells, and ADSC-depleted SVF cell sub-populations.

3.3 Expansion Capacity of ADSC Sub-population after Microfluidic Enrichment

In brief, six vials of cryopreserved SVF cell samples (each vial contained 3×10^6 cells) were thawed in MesenCult™ culture medium and diluted to 30mL in two 15mL centrifuge tubes. After centrifugation at

300×g for 10 minutes, the SVF cell pellet was then re-suspended in culture media. The cell suspension was then filtered with a 40µm pore-size cell strainer to screen out clumps. Upon cell counting with hemocytometer, the SVF cell suspension was re-constituted at a concentration of 1×10^6 cells/mL in 6mL volume. The cell suspension was then used directly for microfluidic sorting without further staining steps.

Cell samples from the collect and discard outlets were collected in 15 mL centrifuge tubes. The cell concentrations from the collect and discard outlet samples were 7×10^4 cells/mL and 1×10^6 cells/mL respectively. The inlet sample without microfluidic enrichment, and collect and discard outlet samples were plated onto a 24-well plate with seeding density of 3×10^5 cells per well. To ensure equivalent cell seeding density in each case, a volume of 2.6mL cell samples from the collect outlet was used in tissue culture. A cell sample volume of 0.18 mL was used in the case of inlet and discard outlet. 2.4 mL culture media was added to the wells in these two cases.

The tissue cultures were incubated at 37°C and 5% CO₂ with multiple passages for one month as shown in Figure S10. As seen from the figure, the initial SVF cultures in Day 0 contained a large number of suspension cells. After overnight culture, most non-attached cells were washed out. Only native ADSCs in the SVF cell mixture which expressed adhesion membrane receptor were able to adhere to the culture well plate. The culture media in each well was then refreshed 2-3 times a week. On Day 4, the adhered ADSCs started to spread and proliferate. At each condition, the tissue cultures were harvested and passaged either at 80% confluency or at two weeks of culture time. At each passage, upon trypsinization with 0.25% Trypsin-EDTA for 10 minutes, the number of harvested ADSCs was counted with a hemocytometer. The harvested ADSCs were then cultured in larger wells or flasks to best match optimized seeding densities. For collect outlet sample, the decrease in the cell population upon P2 was due to uneven cell distribution in P1 tissue culture in the 24-well plate. Adhered cells have a tendency to overcrowd at the edge in smaller 24-well plate. Thus, the cell density was very high near the edge of the 24-well plate with confluency possibly near 100% in P1 culture while in the center of the well the cell confluency appeared to be lower than 80%. Possible cell loss due to centrifugation in cell harvesting also contributed to the decrease in cell counts in P2 and P3. When the cell samples were transferred to 12-well plate, the cells tended to be more evenly distributed in the initial seeding. The ADSCs were able to expand exponentially when using larger 6-well-plate and T25 and T75 flasks in higher passages of P3 to P6 for collect sample.

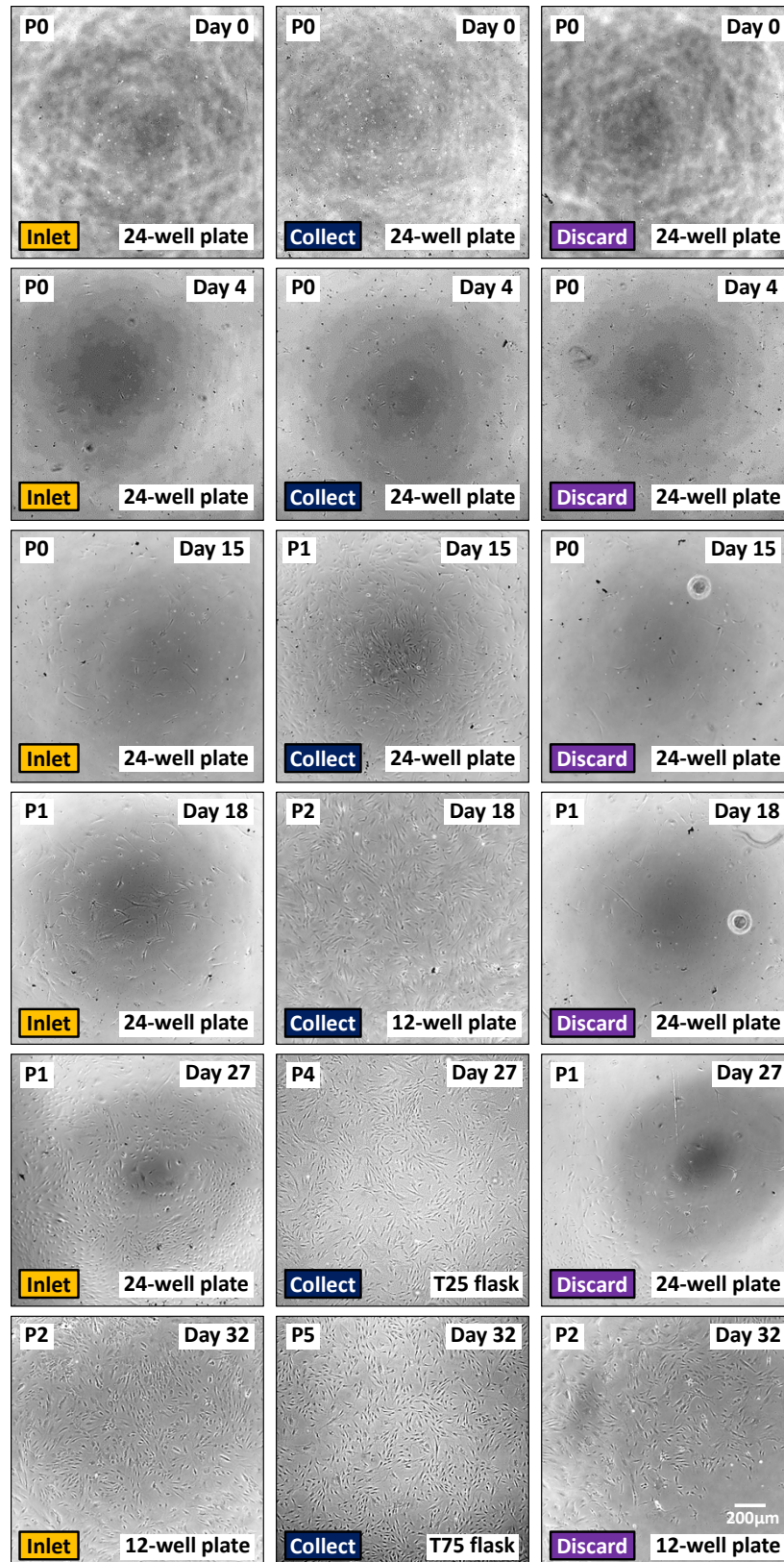


Figure S10. Tissue culture of native human adipose-derived stem cells (ADSCs) isolated from stromal vascular fraction (SVF) cells using continuous cascade integrated microfluidic sorter cascade at multiple passages.

Reference

[1] Zeming, K. K., Salafi, T., Chen, C.-H., & Zhang, Y. Asymmetrical deterministic lateral displacement gaps for dual functions of enhanced separation and throughput of red blood cells. *Scientific Report*, **6**, 22934 (2016).